Supporting Information

Polarization modulated upconversion luminescence: single particle vs few-particle aggregate

Ping Chen, [1] Min Song, [2] E Wu, [2] Botao Wu, [2] Jiajia Zhou, [3] Heping Zeng, [2] Xiaofeng Liu, [1,*] Jianrong Qiu [1,4,*]

[1] School of Materials Science and Engineering, Zhejiang University, Hangzhou 310027, China

[2] State Key Laboratory of Precision Spectroscopy, East China Normal University, Shanghai 200062, China

[3] College of Materials Science and Engineering, China Jiliang University, Hangzhou 310018, China

[4] State Key Laboratory of Luminescent Materials and Devices, South China University of Technology, Guangzhou 510640, China

Contents:

1. Experimental Section

$Y(NO_3)_3 \cdot 6H_2O$ (99.99%), $Er(NO_3)_3 \cdot 6H_2O$ (99.99%) were purchased from Ansheng Inorganic Materials Center (Ganzhou) in China. NaOH, NH_4F, NaF, HNO_3, sodium citrate, EDTA, ethanol, 1-octadecene (90%), and oleic acid (90%) were purchased from Sigma-Aldrich. All of the chemicals were used as starting materials without further purification.

1.1 Synthesis of $NaYF_4$: 5% Er nanodisks

$NaYF_4$: 5% Er nanodisks were prepared with a facile and mild hydrothermal process, in which pH value in the reaction system is critical external parameters for determining the architectural features of the β-$NaYF_4$ nanodisks.[1] In a typical synthesis, an aqueous solution (2.5 mL, 0.2 M) of $Y(NO_3)_3 \cdot 6H_2O$ and $Er(NO_3)_3 \cdot 6H_2O$ (lanthanide ions molar ratio, Y/Er = 95:5) was mixed with an aqueous solution of sodium citrate (22.5 mL. 2.08 M) under stirring for 30 min to form a white solution. Subsequently, aqueous solution (10 mL) of NaF (10 mL, 0.625 M) was added and stirred for 1 h, resulting in a complex with the lanthanide/ sodium citrate/ NaF molar ratio being 1/90/12. Then, HNO_3 was added to adjust the pH of the solution to 3. The obtained solution was then transferred into a 50 mL autoclave and hydrothermally treated at 180 °C for 2 h. After cooling to room temperature, products were separated by centrifugation and washed with ethanol for three times and then dried at 60 °C in vacuum.

1.2 Structural characterizations

X-ray diffraction (XRD) pattern of the dry powder was obtained on a RIGAKU D/MAX 2550/PC diffractometer (Japan) with a slit of 0.02° at a scanning rate of 5° min^{-1} using Cu K_α radiation (λ = 1.5406 Å). Scanning Electron Microscopy (SEM) analysis was performed on a Field Emission Scanning Electron Microscopy (FESEM) (ZEISS SU-8010). High-resolution

Transmission Electron Microscopy (HRTEM) analysis was performed on a FEG-TEM (Tecnai G2 F30 S-Twin, Philips-FEI, Netherlands) operated at 300 kV.

2. Supplementary date

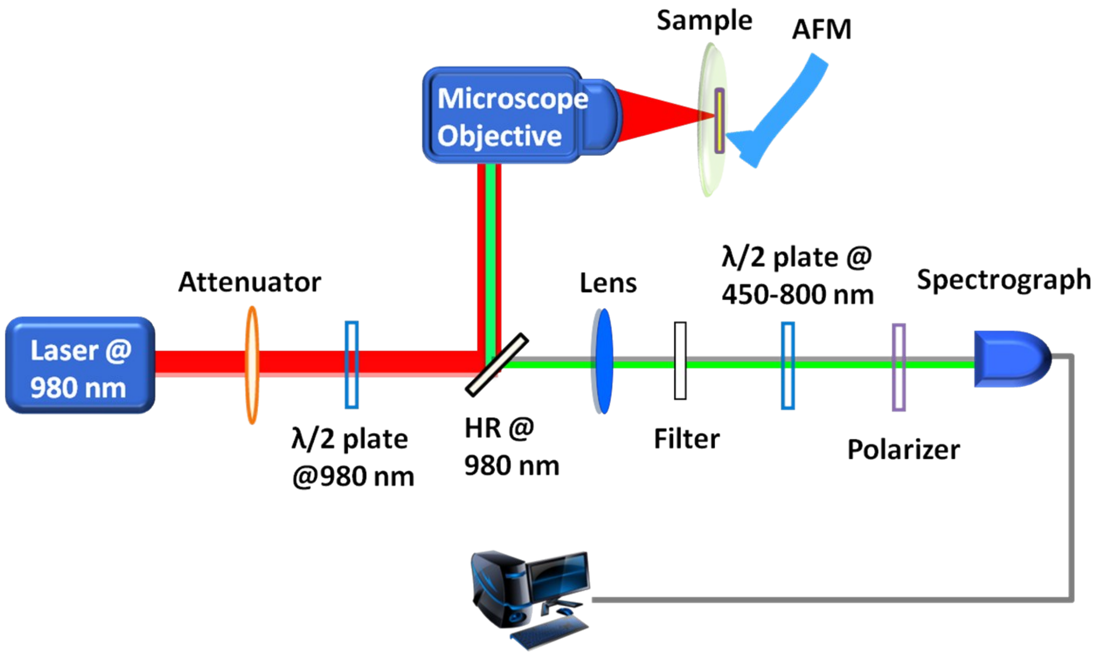

Fig. S1 Schematic diagram of luminescence spectrum test system.

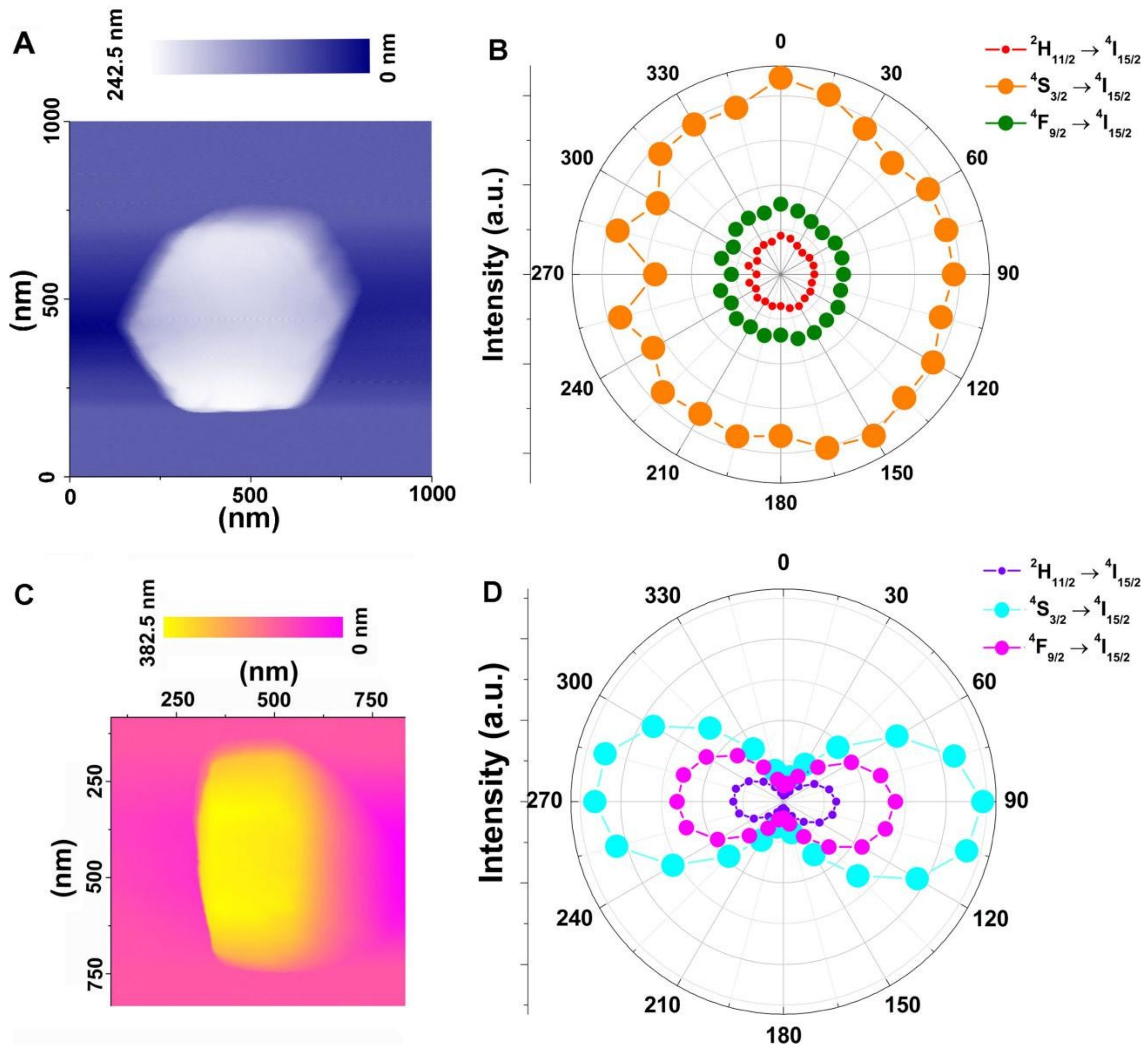

Fig. S2 A) AFM images of single nanodisk recorded for a single nanodisk in which the *a* axis is parallel to the horizontal plane (HP). B) Polar plots of integrated UC luminescence intensity of single nanodisk as a function of excitation polarization angle for the transitions from $^2H_{11/2} \rightarrow {}^4I_{15/2}$, $^4S_{3/2} \rightarrow {}^4I_{15/2}$, $^4F_{9/2} \rightarrow {}^4I_{15/2}$ of Er^{3+}, recorded at *a* // HP and E_{ex} // *a* axis @ θ = 0°. C) AFM images of single nanodisk recorded for a single nanodisk in which the *c* axis is parallel to HP. D) Polar plots of integrated UC luminescence intensity of single nanodisk as a function of excitation polarization angle for the transitions from $^2H_{11/2} \rightarrow {}^4I_{15/2}$, $^4S_{3/2} \rightarrow {}^4I_{15/2}$, $^4F_{9/2} \rightarrow {}^4I_{15/2}$ of Er^{3+}, recorded at *c* // HP and E_{ex} // *c* axis @ θ = 0°.

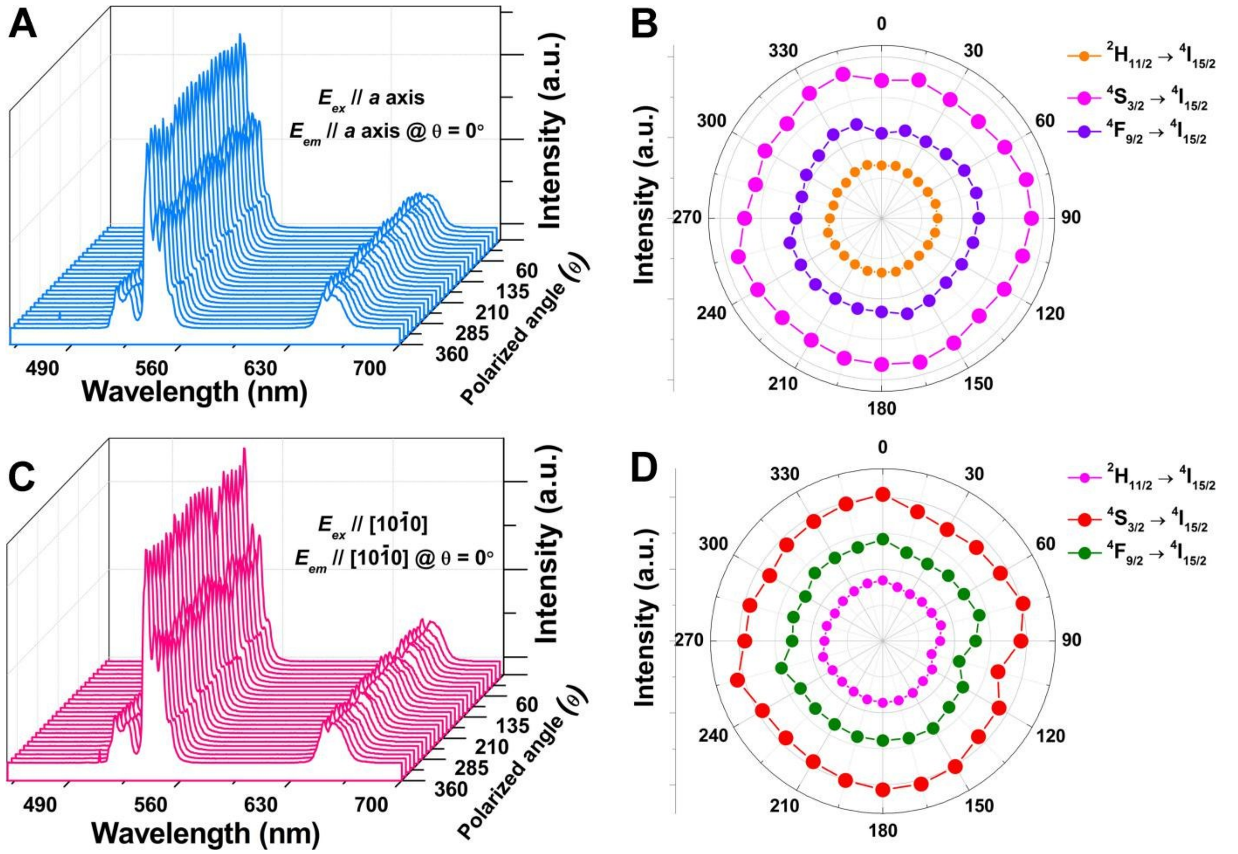

Fig. S3 A) UC luminescence spectra recorded at emission polarization angles of 0° - 360° for single nanodisk under conditions of *a* // HP and E_{ex} // *a*. B) Polar plots of integrated UC luminescence intensity as a function of emission polarization angle for the transitions from $^2H_{11/2} \rightarrow {}^4I_{15/2}$, $^4S_{3/2} \rightarrow {}^4I_{15/2}$, $^4F_{9/2} \rightarrow {}^4I_{15/2}$ of Er^{3+} for single nanodisk under configurations of *a* // HP and E_{ex} // *a*. C) UC luminescence spectra recorded at emission polarization angles of 0° - 360° for single nanodisk under conditions of *a* // HP and E_{ex} // [10**Error!**0]. D) Polar plots of integrated UC luminescence intensity as a function of emission polarization angle for the transitions from $^2H_{11/2} \rightarrow {}^4I_{15/2}$, $^4S_{3/2} \rightarrow {}^4I_{15/2}$, $^4F_{9/2} \rightarrow {}^4I_{15/2}$ of Er^{3+} for single nanodisk under configurations of *a* // HP and E_{ex} // [10**Error!**0].

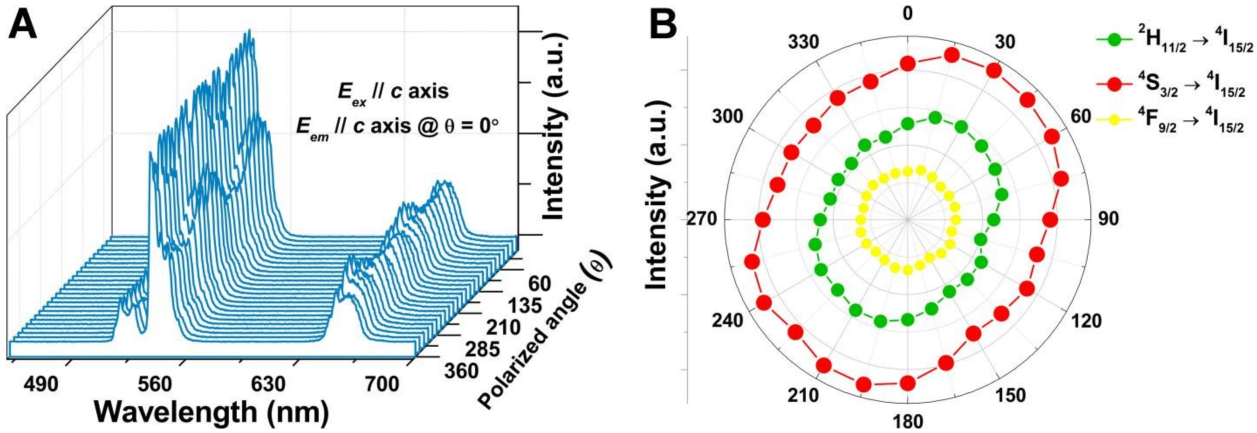

Fig. S4 A) UC luminescence spectra recorded at emission polarization angles of 0° - 360° for single nanodisk under conditions of *c* // HP and E_{ex} // *c*. B) Polar plots of integrated UC luminescence intensity as a function of emission polarization angle for the transitions from $^2H_{11/2} \rightarrow {}^4I_{15/2}$, $^4S_{3/2} \rightarrow {}^4I_{15/2}$, $^4F_{9/2} \rightarrow {}^4I_{15/2}$ of Er^{3+} for single nanodisk under configurations of *c* // HP and E_{ex} // *c*.

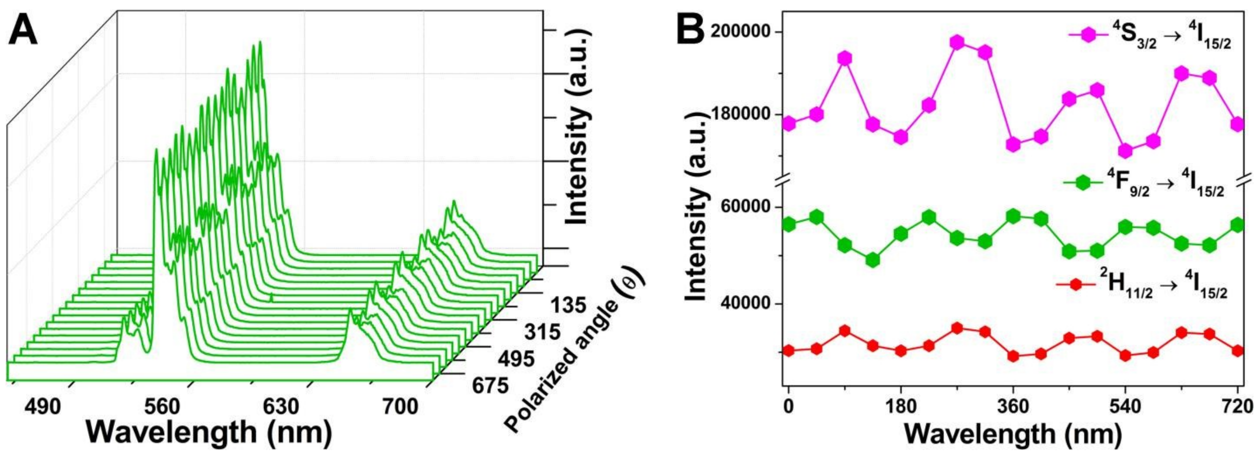

Fig. S5 A) UC luminescence spectra of the aggregated nanodisks recorded under emission polarization angle varied from 0° to 360°. C) The dependence of UC luminescence intensity of the aggregated nanodisks with different transitions of Er^{3+} on the emission polarization angle.

Reference

1. L. Liang, Y. Liu, C. Bu, K. Guo, W. Sun, N. Huang, T. Peng, B. Sebo, M. Pan, W. Liu, *et. al. Adv. Mater.*, 2013, **25**, 2174.